

Review

Nano/Microrobots Line Up for Gastrointestinal Tract Diseases: Targeted Delivery, Therapy, and Prevention

Lukáš Děkanovský, Jinhua Li, Huaijuan Zhou, Zdenek Sofer and Bahareh Khezri * 

Department of Inorganic Chemistry, University of Chemistry and Technology Prague, Technická 5, 16628 Prague, Czech Republic; dekanovl@vscht.cz (L.D.); lii@vscht.cz (J.L.); zhoubu@vscht.cz (H.Z.); soferz@vscht.cz (Z.S.)

* Correspondence: bahareh.khezri@vscht.cz or bahareh.khezri.research@gmail.com

Abstract: Nano/microrobots (NMRs) are tiny devices that can convert energy into motion and operate at nano/microscales. Especially in biomedical research, NMRs have received much attention over the past twenty years because of their excellent capabilities and great potential in various applications, including on-demand drug delivery, gene and cell transport, and precise microsurgery. Reports published in recent years show that synthetic nano/microrobots have promising potential to function in the gastrointestinal (GI) region, particularly in terms of drug delivery. These tiny robots were able to be designed in such a way that they propel in their surroundings (biological media) with high speed, load cargo (drug) efficiently, transport it safely, and release upon request successfully. Their propulsion, retention, distribution, and toxicity in the GI tract of mice has been evaluated. The results envisage that such nano/microrobots can be further modified and developed as a new-generation treatment of GI tract diseases. In this minireview, we focus on the functionality of micro/nanorobots as a biomedical treatment system for stomach/intestinal diseases. We review the research progress from the first in vivo report in December 2014 to the latest in August 2021. Then, we discuss the treatment difficulties and challenges in vivo application (in general) and possible future development routes.

Keywords: nano/microrobots; biomedical applications; imaging; stomach diseases; micromotors; microswimmers; drug delivery



Citation: Děkanovský, L.; Li, J.; Zhou, H.; Sofer, Z.; Khezri, B. Nano/Microrobots Line Up for Gastrointestinal Tract Diseases: Targeted Delivery, Therapy, and Prevention. *Energies* **2022**, *15*, 426. <https://doi.org/10.3390/en15020426>

Academic Editor: Peter Foot

Received: 21 October 2021

Accepted: 4 January 2022

Published: 7 January 2022

Publisher's Note: MDPI stays neutral with regard to jurisdictional claims in published maps and institutional affiliations.



Copyright: © 2022 by the authors. Licensee MDPI, Basel, Switzerland. This article is an open access article distributed under the terms and conditions of the Creative Commons Attribution (CC BY) license (<https://creativecommons.org/licenses/by/4.0/>).

1. Introduction

In 1966, the science fiction ‘Fantastic Voyage’ [1] used an example of a famous speech of Richard Feynman ‘There is plenty room at the bottom’, delivered in 1959 [2]. He talked about smart tiny devices that can be swallowed, swim through blood vessels, and remove damaged parts, and then the movie presents a submarine that is shrunk to the size of a microbe to fix the clot on a mission to rescue a scientist. The idea of using nano/microrobots (NMRs) for biomedical applications was mostly initiated by these two events [1,2]. As nanotechnology boundaries have been pushed, scientists and researchers have developed tiny robots and presented many “proof-of-concept” and “preliminary demonstration” studies over the past 20 years.

NMRs made from or coated with functionalized and appropriate materials have the ability to swim using either a chemical fuel presented ideally in the same environment or an external source. Since the first report on rod-shaped Au/Pt nanomotors driven by the hydrogen peroxide catalytic reaction, [3] this research field has progressed extensively to achieve nano/microrobots with a sophisticated design capable of performing complex tasks. Different materials have been used to achieve these goals, including polymers [4,5], two-dimensional materials [6,7], metal–organic frameworks (MOFs) [8], and hybrid materials [9]. In addition, many efforts have been made to use different catalytic reactions [4–6] or integrate components that respond to an external energy source (magnetic field [7], electrical

field [8], acoustic wave [9], and light [10]) and allow them to be controlled remotely. Since then, many proof-of-concept studies have been reported in various fields such as biomedical [11,12], environmental [13], defense, and food safety [14,15] demonstrating the high potential and feasibility of NMRs in real applications. Their small size and mobility make them promising tools with versatile applications in the biomedical field. For example, in recent decades, localized drug delivery systems have received significant attention due to the high demand for efficient functionality and a reduction in the side effects of therapy [16]. The challenges of the accompaniment of targeted drugs in clinical practice are the following: (i) finding the target in a specific disease, (ii) finding a drug which can cure/prevent it, and (iii) having a drug carrier capable of reaching the target safely. NMRs have shown that they can function as an active and promising self-propelled platform for drug delivery [17–21]. These tiny robots combine the benefits of traditional carriers such as drug protection, selectivity, and biocompatibility with their ability to swim and penetrate into the targeted tissues and release the drug at the desired time and location. To accomplish the task of NMR-based drug delivery, high power is required to drive the robots, control motion and navigate through the predefined pathways. To achieve efficient pickup, transport, and delivery of drugs, a specific interaction between robots and drugs (e.g., electrostatic and hydrogen bonding) is required. In particular, the latest advances in the architecture and development of motors have led to great achievements in the driving force, manipulated motion, velocity, and functionality of the outer layer of tiny motors [17–21]. In addition to targeted drug delivery, NMRs have been used successfully for sampling and biopsy [22], imaging [23–25], tissue engineering [26], detoxification treatments [27,28], gene and cell delivery [29,30], and biofilm degradation [31,32].

Although these studies are mainly in their early stages, it is expected that in the near future NMRs will travel through the body and replace current traditional treatments that face difficulty accessing certain organs. We believe that significant advances have been made, but we are still far from where we should be, and this is mainly due to a lack of clinical studies. In fact, researchers still face some key challenges, such as biocompatibility and biodegradability, tracking and positioning, imaging, and bio barriers that need to be overcome prior to the realization of this technology. Most of these reports are classified as proof-of-concept and preliminary studies that propose basic concepts and are limited in practical applications. For example, a large portion of the reported bubble-propelled NMRs consume hydrogen peroxide, which is not a biocompatible fuel. An alternative is to design NMRs that can be propelled due to the reaction with substances existing in the body such as glucose, water, acid, urea, and other physiological liquids as fuels [4,6,33–35]. For example, Sanchez et al. [36] reported the swarming behavior of silica-based nanorobots powered by urease. The nanorobots were labeled with iodine-124 and fluorine-18. The biodistribution of nanorobots was investigated in a mouse model and the results confirmed the suitability of positron emission tomography (PET) as an in vivo tracking and positioning method, as well as the stability of the radiochemical labels. The swarming behavior of nanorobots has also been explored in the bladder of mice [36]. These works open up a path in bladder cancer therapy. Ultrasound-guided Mg-based and NIR-responsive Cyanobacteria microrobots have also been developed for the treatment of rheumatoid arthritis [37,38]. The ability of reported microrobots for the treatment of rheumatoid arthritis was evaluated using collagen-induced arthritis rats and the results reveal that inflammation was significantly reduced [37,38]. These findings *propose examples for the potential application of NMRs as active H₂/O₂ generators in the treatment of various inflammatory diseases. The same concept is also used for the precise in vivo therapy of acute ischemic stroke. Mg-based microrobots generate hydrogen while swimming and by delivering active H₂ were able to improve intracellular reducibility [39].

Helicobacter pylori is considered one of the most common bacterial infections. Studies show that in most cases it is responsible for inflammatory gastritis [40], stomach ulcers [41,42], extragastric diseases [43,44], and the risk of gastric cancer [45]. The traditional standard treatment of *H. pylori* infection is a three-course therapy that requires

the prescription of two antibiotics (clarithromycin and amoxicillin/metronidazole) and a proton pump inhibitor (PPI) [42]. It has been shown that prolonged treatment with multiple broad-spectrum antibiotics and proton pump inhibitors causes other health complications [46]. The reported diseases associated with long-term use of PPIs in the literature are *C. difficile* infection, dementia, pneumonia, antiplatelet agents, kidney disease, micronutrients, and bone mineral density deficiency [46]. Long-term administration of antibiotics also has adverse effects on beneficial bacteria and also resistance to further treatment using the same antibiotics. These adverse side effects of traditional medicine and their nontargeting effects urge us to look for an effective vaccine and alternative therapeutic options [33,47].

This review aims to highlight in vivo reports using NMRs that have a profound impact on the treatment of gastrointestinal (GI) tract disease. We will describe and discuss the progress made in past years for the design of effective biocompatible nano/microrobots toward efficient biomedical tasks in vivo including pH neutralization, precise penetration to the stomach wall, drug delivery, and imaging (Scheme 1). These microrobots are listed in Table 1.



Scheme 1. Schematic of reported in vivo treatment and imaging of stomach diseases using nano/microrobots. (A) Invented oral medicine based on nano/microrobots for prevention (vaccine) and treatment (tablet) of stomach diseases, (B) presenting the morphology of the reported nano/microrobots employed for treatment of stomach diseases and imaging. (C) Presenting the means used to propel nano/microrobots in the treatment of stomach diseases.

Table 1. List of reported studies employing NMR for in vivo stomach/intestinal treatment.

NMR	Organ (In Vivo)	Propulsion Mode	Responsibility	Size	Velocity (μms^{-1})	Ref
PEDOT/Zn	Stomach	Acid powered (gastric juice)	cargo delivery	5 μm	60	[48]
Enteric coating/PEDOT/Au/Mg	Intestine	Intestinal fluid powered	Deliver the payload to a particular location to localize tissue penetration and retention.	5 μm	60	[49]
pH-sensitive polymer/Au/Mg	Stomach	Acid powered (gastric juice)	The neutralization of gastric environment and cargo delivery	20 \pm 5 μm	60	[50]
Chit/PLGA/TiO ₂ /Mg	Stomach	Acid powered (gastric juice)	Antibiotic delivery for H. pylori infection and neutralization of the acidic environment	20 \pm 5 μm	120	[47]
Mg/TiO ₂	Stomach	Acid powered (gastric juice)	Targeted cargo delivery	20 \pm 5 μm	~300	[51]
pH-sensitive polymer/PEDOT/Au/Zn/	Stomach	Acid powered (gastric juice)	Targeted cargo delivery	5 μm	70	[52]
Spirulina platensis/Fe ₃ O ₄	intraperitoneal cavity	Magnetic field	Imaging	~200 μm	-	[53]
Si Nanobottles	Stomach	Acid powered (gastric juice)	Antibiotic delivery for H. pylori infection and neutralization of the acidic environment	576 \pm 50 nm	-	[54]
PDA MC	Stomach	Urea powered	Penetration and retention in the stomach wall	1 μm	0.78–1.9	[55]

2. Nano/Microrobots (NMR) in Action for Stomach Diseases

2.1. Zinc (Zn)-Based NMRs

Wang et al. [48] reported the first in vivo study of synthetic Zn-based microrobots using a live mouse model. Microrobots were fabricated using the electrochemical deposition method using Cyclopore polycarbonate membrane templates (Figure 1A). PEDOT/Zn microrobots were prepared as follows: (I) deposition of the poly (3,4-ethylenedioxythiophene (PEDOT) microtube, (II) deposition of the inner zinc layer, and (III) dissolution of the membrane and release of the microrobots. The resulting PEDOT/Zn microrobots were able to swim autonomously in the simulated gastric fluid (pH = 1.2) as Zn participated in a redox reaction, oxidized, and ejected H₂ bubbles ($\sim 60 \mu\text{ms}^{-1}$). Their retention properties were examined using a mouse model. In this regard, PEDOT/Zn microrobots are compared with PEDOT/Platinum (Pt) microrobots (they could not move in gastric juice). The results reveal that after two hours, a large number of PEDOT/Zn microrobots were observed on the stomach wall, while in the control experiment the retention of the PEDOT/Pt microrobots on the stomach wall was significantly lower. It was shown that the propulsion of Zn-based microrobots in the acid environment of the stomach facilitated their penetration and retention in the porous, gel-like mucus layer of the stomach wall. As time increased, the number of retained microrobots decreased due to their degradation and transfer to the small intestine (Figure 1B).

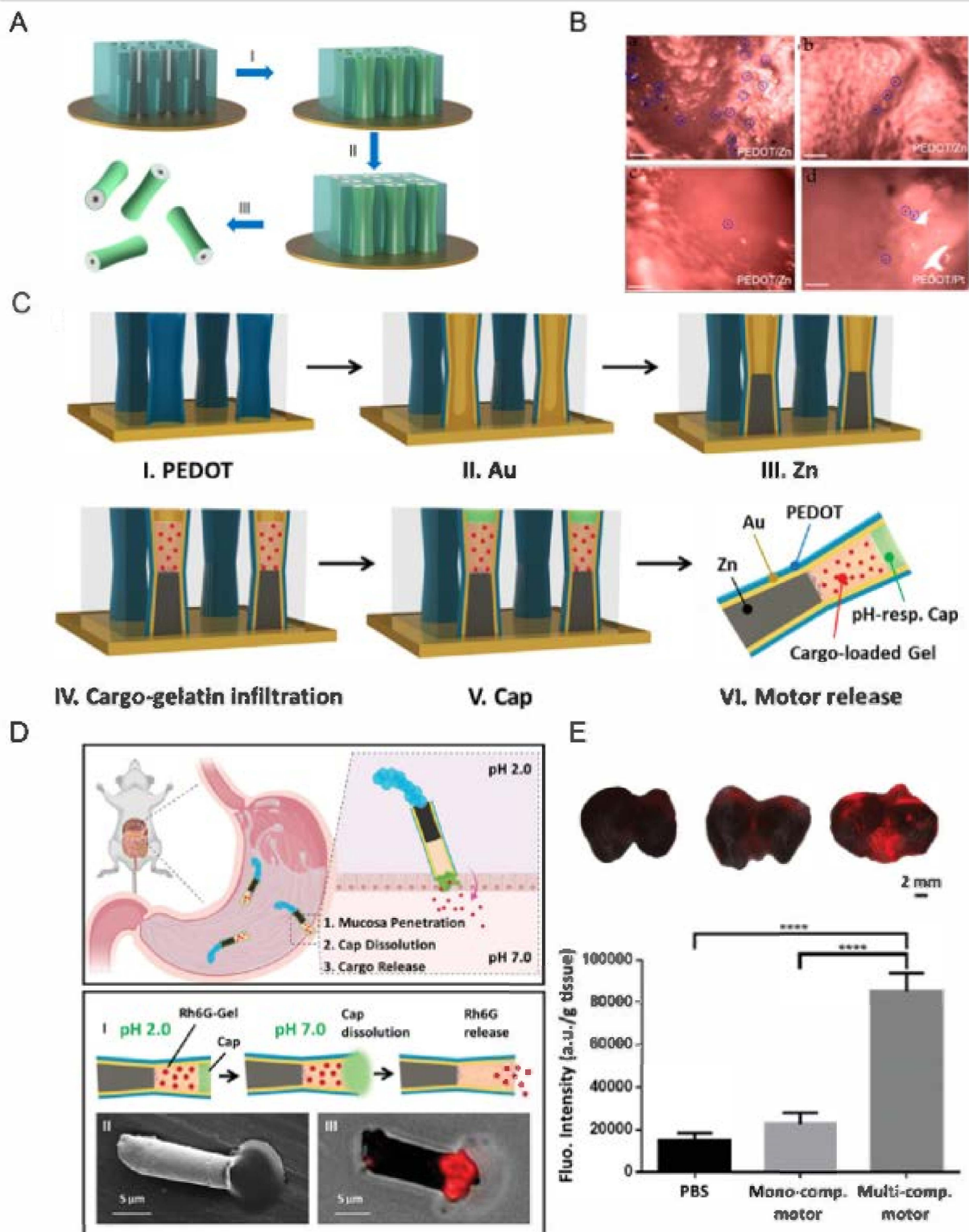


Figure 1. Zn-based NMRs. (A) Preparation of PEDOT/Zn microrobots: (I) deposition of the PEDOT microtube, (II) deposition of the inner zinc layer, and (III) dissolution of the membrane and release of the micromotors. (B) Microscopic images illustrate the retained micromotors in the stomach tissues collected at (a) 2 h, (b) 6 h, and (c) 12 h post-oral administration of PEDOT/Zn micromotors and (d) 2 h post-oral administration of PEDOT/Pt micromotors (serving as a negative control). Scale bars, 100 μ m. (Reproduced with permission from Ref. [48], Copyright © 2014 American Chemical Society.) (C) Schematic of the preparation of the multicompartment motor: (I) PEDOT electropolymerization;

(II) Au electrodeposition; (III) galvanostatic electrodeposition of Zn; (IV) cargo-loaded gelatin infiltration for 20 min at 50 °C; (V) protective cap using 8% Eudragit L100 polymer, and (VI) release of the multicompartment motor by dissolving the polycarbonate membrane template. (D) Top panel: Schematic of the propulsion and distribution of the multicompartment motors in a mouse stomach along with the efficient tissue penetration, dissolution of the enteric coating, and responsive release of the cargo in the gastric lining. Bottom panel: Schematic of the dissolution of the enteric cap, along with the release of the Rh6G cargo from the multicompartment motor (I); SEM (II) and merged microscopy (III) images showing the release of the Rh6G-loaded gelatin from the multicompartment motor. (E) Top (from left to right): merged images of the luminal lining of freshly excised mouse stomach at 2 h after oral gavage of PBS (control), monocompartment motors and multicompartment motors. Bottom: corresponding fluorescence quantification of the three groups. Error bars calculated as a triple of s.d. ($n = 3$) (**** $p < 0.0001$). (Reproduced with permission from Ref. [52], published by John Wiley and Sons, 2020.).

The capability of PEDOT/Zn tubular microrobots for cargo delivery was also tested. In this regard, AuNPs were loaded into the PEDOT/Zn microrobots prior to zinc electrodeposition. As Zn dissolved gradually in the gastric environment, AuNPs were released. The retention of Au NPs released from PEDOT/Zn microrobots on the stomach wall was compared with the retention of Au NPs administered orally, indicating that the same result was obtained. The PEDOT/Zn microrobots were able to deliver a large amount of the Au NPs because of their motion. These observations evidently confirm the importance of being active (self-propulsion) for efficient delivery. This work considers pioneering and opens avenues for diagnostics, imaging, and treatment for various scenarios. The great advantage was the biodegradation of PEDOT/Zn microrobots upon completion of their task. Lastly, clinical tests showed that PEDOT/Zn tubular microrobots do not leave any toxic products by swimming, delivering the cargo, and dissolving in gastric juice.

Recently, the same research group [52] developed a new multicompartment Zn-based microrobot. These microrobots were fabricated using the template-assisted electrodeposition method (Figure 1C), in which the tubes include two caps: (i) Zn acting as a swimming engine and (ii) pH-responsive polymer that protects the loaded cargo and releases the cargo in response to its environmental pH change. The longer lifetime of the microrobot was achievable by increasing the Zn electrodeposition time. The dissolution time of the polymeric coating can also be altered by the thickness of the polymer. As combinatorial therapy has been preferred due to the synergistic effect of multiple drugs, the possibility of loading multiple cargoes in different compartments of the same microrobot was explored. Two different cargoes, including iron and silver nanoparticles, were selected as model cargoes. The microrobots were characterized in terms of structure, swimming, safe cargo loading, and release processes in vitro followed by in vivo tests using a mouse model (Figure 1D). Microrobots were loaded with Rhodamine 6G (Rh6G) as model cargo. The microrobot propels as a result of the catalytic reaction happening between Zn and gastric juice, swims toward the stomach wall where the front end penetrates the stomach tissue, the enteric polymeric cap is dissolved, and the therapeutic cargo is released. The results also demonstrate that this multicompartment robot is much more effective than the monocompartment previously designed, and no toxic residue was observed. The enhanced distribution and retention of the multicompartment microrobots could be the result of their novel design (Figure 1E). It seems that the cap only dissolves once it reaches the stomach wall and penetrates the mucosal lining, which means higher pH. Thus, there is likely to be no Rh6G leakage in the acidic area. In the case of monocompartment microrobots, the cargo is not protected, and gradual leakage is possible. The unique properties of these reported microrobots, including fast propulsion in an acidic environment, high loading capacity, the possibility of loading multiple cargoes, autonomous delivery, their biocompatibility, and biodegradability, offer great promise for gastric targeted drug delivery using NMRs.

2.2. Magnesium (Mg)-Based NMRs

Magnesium-based NMRs are also similar to Zn-based robots. They can directly use their surrounding medium (aqueous) as fuel to produce H₂ bubbles for swimming. These robots eliminate the need for commonly used toxic fuels. Mg-based microrobots have been designed in tubular and Janus shapes for the treatment of stomach diseases.

Wang et al. [49] reported a tubular PEDOT/Au robot used as a container to load Mg particles and the cargo model (Au NPs) inside (Figure 2A). The microrobots were covered with an enteric polymer as a protection layer against gastric juice. This polymeric layer is stable in an acid environment (pH 1–3) while it dissolves in neutral and alkaline media (pH 6–7), which allows robots to deliver cargo safely. The thickness of the polymeric layer can be tuned according to the time required for the travel of the robot through the gastrointestinal tract before its propulsion is activated. The results show that the dissolution of the polymer and the propulsion of the robots took around 10 min for a thin coating (0.3 µm), while for a medium (0.8 µm) and thick (1.2 µm) coating, the robot activation was much slower, 30–40 min and 3 h, respectively. Interestingly, for each thickness of the polymeric coating, activation occurred in different segments (upper, middle, and lower) of the gastrointestinal tract (GI). These results prove that, by controlling the coating thickness, the positioning of the robots can be selected in different regions of the GI. The functionality of these robots was examined in a mouse model (oral administration), and the *in vivo* results show that Mg-based microrobots swam securely through the gastric fluid and were activated in the GI tract. Like Zn-based robots, it was expected that the propulsion of Mg-based robots increases local retention and penetration because of their swimming and trapping in the mucus layer. In this regard, the PEDOT/Au robot loaded with the Mg was compared with silica microsphere-loaded (no propulsion). The results show that the fluorescence intensity of the inactive robots (loaded with silicone) is much lower than that of those loaded with Mg. This confirmed that penetration improved due to propulsion (Figure 2A). Retention has been estimated to last up to 24 h. The toxicity profile of robots in the GI tract does not reveal any significant damage to the system.

The same research group [50] developed an Mg-based multifunctional Janus micro-robot that offers swimming, acid neutralization, loading, transport, and payload release in response to pH changes (Figure 2B, right panel). Mg particles were dispersed on the glass slide, coated with Au, and then the particles were covered with the pH-sensitive coating (EUDRAGIT®L100-55, dissolves at pH > 5.5). This design leaves a small opening to expose Mg to the surrounding environment for propulsion. Once the Mg-based microrobot entered the stomach, Mg reacted with gastric juice, hydrogen bubbles formed, and the microrobot started to swim. The response of the Mg microrobot core to acid causes rapid proton depletion that neutralizes the acidic environment. Furthermore, due to a change in pH, therapeutic cargos could be released [50]. The mice were treated with 5 mg of Mg-based NMRs to evaluate their ability to (i) neutralize gastric acid, (ii) activate the dissolution of the pH-responsive polymeric coating and then (iii) release the payload. Mice treated with water and PS particles were used as a control. Fluorescence images confirmed that Mg-based NMRs can actively adjust the pH of the stomach environment to facilitate the dissolution of the pH-sensitive polymer and the release of the payload compared to controls (Figure 2B left panel, top). Inert PS particles showed almost the same results as water and did not alter the pH of the stomach. Subsequently, mice were treated with Mg-based NMRs, and fluorescence imaging was employed to evaluate pH recovery over time. Twenty minutes after administration, the fluorescence intensity was strong, while 24 h later indicated a very low intensity (Figure 2B, left panel, bottom). These studies open the door to the use of NMRs as active delivery platforms for the *in vivo* therapeutic treatment of stomach diseases, while they can create the functional environment required [47–50].

In their next work [47], a similar design of Mg-based microrobots (Janus), loaded with clarithromycin (an antibiotic), was used for the first time for the treatment of bacterial stomach infection (*H. pylori*) *in vivo* (tested in mice). Antibiotics loaded in polylactic glycolic acid (PLGA) on top of the Mg core were protected with the Ti layer, and then

everything wrapped in chitosan that aided the stickiness of the microrobots to the stomach wall. These microrobots were able to reduce and neutralize the acidity of their swimming environment in 20 min. Rapid proton depletion occurs due to the consumption of protons by microrobots while propelling within the stomach. In vivo tests showed that these Mg-based microrobots can complete their task safely and without any change in stomach function. Their findings show that the original stomach acidity can be restored after 24 h of robot administration. One of the promising aspects of using Mg-based microrobots for *H. pylori* infection was the completion of treatment without the need for the administration of proton pump inhibitors such as omeprazole, pantoprazole, and rabeprazole. Long-term administration of proton pump inhibitors causes adverse side effects, e.g., headache, diarrhea, constipation, fever, vomiting, and nausea. These microrobots combined acid neutralization with the treatment task.

Although oral administration would be preferred due to its simplicity and convenience, and is usually the safest and least expensive, these pioneering works have employed microrobots for in vivo studies via injection. Oral administration of robot-based active drug delivery systems is limited because of their fast catalytic reaction with the surrounding environment. In this regard, Wang et al. introduced a microrobot tablet that can be taken orally [51]. This microrobot tablet contained Janus microrobots based on Mg introduced in their previous works [47,50] that dispersed uniformly in the matrix of the tablet (lactose/maltose, cellulose/starch) (Figure 2C, left panel, top). The distribution of the tablet matrix was evaluated using three different tablet sizes (small, 2×3 mm, medium, 3×3 mm, and large, 5×3 mm). The microrobot is activated upon disintegration and dissolution of the tablets, which is a function of size and temperature. The disintegration time was shorter at higher temperatures. In this study, the effect of additives commonly used in the pharmaceutical industry was tested. The addition of small amounts of cellulose and starch derivatives increased the dissolution speed of the microrobot tablets due to the rapid water adsorption and swelling that facilitate tablet disintegration. To evaluate the in vivo function of the introduced tablets, they were administered orally to a mouse model. Consequently, the microrobot fabricated using a model cargo was loaded into PLGA and coated with chitosan as a functional external layer to enhance the penetration of the robots. The results show that the microrobots can reach the stomach safely using the introduced platform. The tablet was encapsulated in the area of the gastrointestinal tract and the microrobots swam in the gastric juice (Figure 2C, right panel). Tablets containing Mg-based microrobots were compared with those prepared using Si instead of Mg particles and free Mg-based robots. The highest fluorescence intensity corresponded to tablets containing Mg-based microrobots, which confirmed the ability of microrobot tablets in a more concentrated manner compared with colloidal form administration and also tablets loaded with inactive microparticles (Si) (Figure 2C, left panel, bottom) [51]. This work not only offered convenient oral administration, but biocompatible microrobot tablets also offer better control of dosage and activity.

As most infections begin in the mucosal layer or involve it, the development of a mucosal vaccine against a variety of bacteria is highly demanded. Usually, vaccination is considered as an efficient method to preventing infectious diseases. In this regard, the development of a vaccine with powerful and effective formulation, easy administration, and higher levels of adherence is highly desirable. One of the examples is common stomach infections caused by *Helicobacter pylori*, *E. coli*, etc. In this regard, the development of vaccines can promote mucosal immunity that does not allow bacteria and viruses to bind and penetrate the mucosal layer. Wang et al. [56] developed a robot-based vaccine using previously reported Mg-based robots. Consequently, Mg microparticles coated with a layer of TiO_2 were fabricated using atomic layer deposition (ALD).

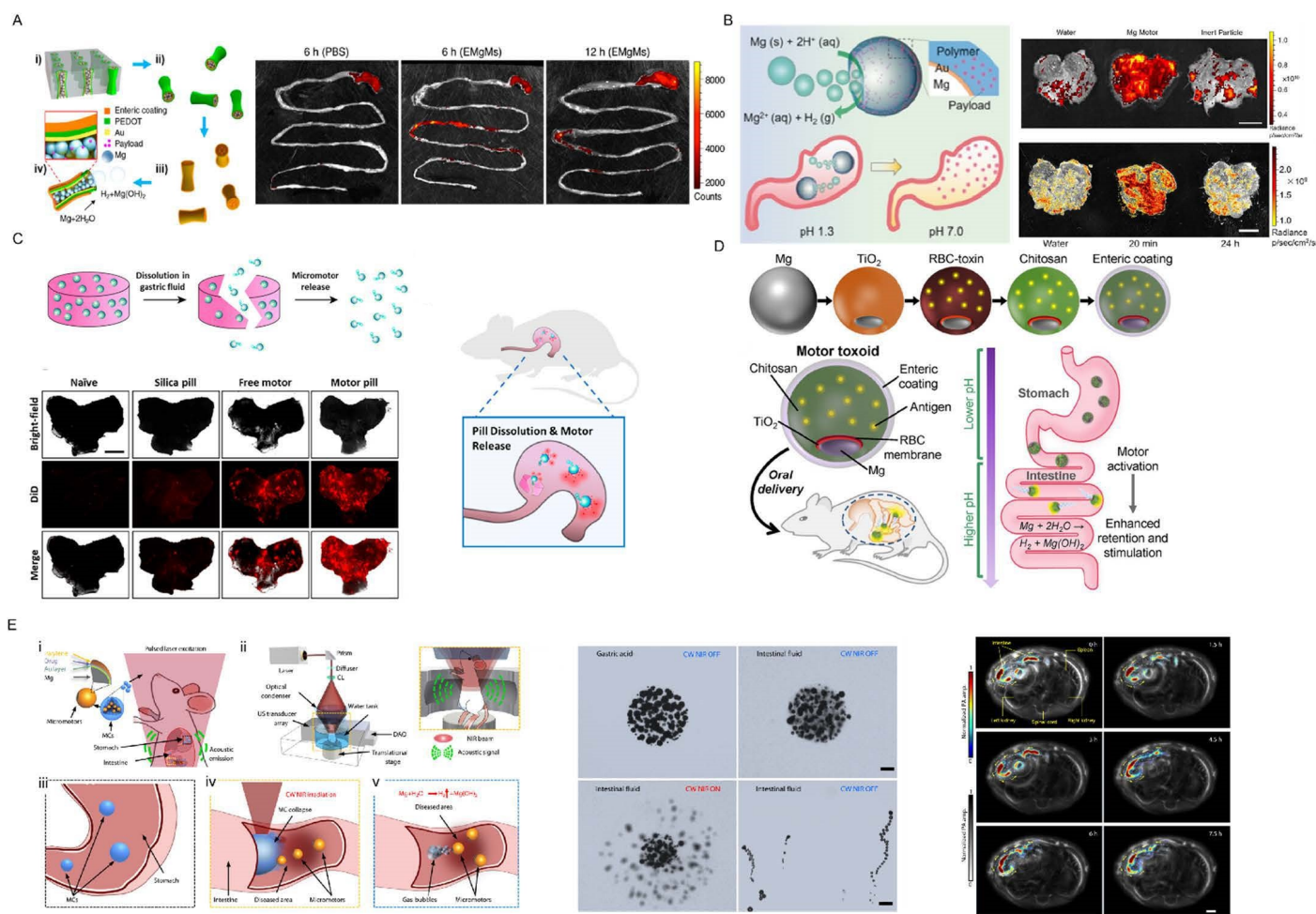


Figure 2. Mg-based MNRs. (A) Left panel: Preparation of Mg-based micromotors: (i) loading of Mg microspheres and payload into PEDOT/Au microtubes electrodeposited in microporous polycarbonate (PC) membrane with a pore size of 5 μm and pore length of 15 μm ; (ii) dissolution of the PC membrane and release of the Mg micromotors; (iii) coating Mg micromotors with enteric polymer; (iv) dissolution of the enteric coating and propulsion of Mg micromotors in solution with neutral pH. Right panel: Superimposed fluorescent images of mouse GI tracts at 6 and 12 h post-administration of microrobots loaded with the dye Rhodamine 6G and covered with medium polymer coating. Phosphate-buffered saline was used as a control (reproduced with permission from Ref. [49], Copyright © 2016 American Chemical Society). (B) Left panel: Illustrations of an acid-powered Mg-based microrobot and its acid neutralization mechanism. The micromotor is made of a Mg microsphere coated with a thin gold (Au) layer and a payload-encapsulated pH-sensitive polymer layer. At acidic pH, the Mg reacts with acids and generates hydrogen bubbles, thus propelling the motors and depleting protons in the solution. Right panel (top): Superimposed fluorescent images, of the whole stomach of mice, collected 20 min post-administration of DI water, Mg micromotors, and inert PS microparticles (both Mg micromotors and PS microparticles are loaded with DiD dye, which is encapsulated within the pH-sensitive polymer coating as a model drug). Right panel (bottom): Fluorescent images of the pH indicator BCECF superimposed on the entire stomach for the 20 min and 24 h post-administration of 5 mg of the Mg micromotor. Mice treated with water were used as a control (reproduced with permission from Ref. [50], published by John Wiley and Sons, 2017) (C) Left panel (top): Schematic of micromotor pill dissolution in gastric fluid and subsequent micromotor release. Left panel (bottom): Bright-field, fluorescent (DiD dye loaded onto the micromotors), and merged images of the luminal lining of freshly excised mouse stomachs at 4 h after oral gavage of DI water (naïve), using DiD-loaded silica pills, free DiD-loaded Mg-based micromotors, or DiD-loaded Mg-based micromotor pills. Scale bar, 5 mm. Right panel: Schematic in vivo actuation of a micromotor

pill (not to scale): pill dissolution in gastric fluid, micromotor release, and distribution of fluorescent cargoes in mouse stomach tissue (reproduced with permission from Ref. [51], Copyright © 2018 American Chemical Society). (D) Schematic of micromotor toxoids for oral vaccination. Top panel: Motor toxoids are fabricated by a sequential process in which magnesium (Mg) microparticles are coated with an asymmetrical layer of TiO₂, followed by a toxin-inserted RBC membrane (RBC-toxin) as the antigenic material, mucoadhesive chitosan, and a pH-sensitive enteric coating. Bottom panel: When administered orally to mice, motor toxoids first enter the stomach, where the enteric coating protects the formulation from degradation in the low pH environment. With the more neutral pH of the intestine, the enteric coating dissolves and the intestinal fluid activates the motors. The autonomous propulsion of the motors enables enhanced retention and penetration in the intestinal wall, enhancing immune stimulation against the antigenic payload (reproduced with permission from Ref. [56], Copyright © 2019 American Chemical Society). (E) Left panel: Schematic of PAMR in vivo. (i) Schematic of the PAMR in the GI tract. The MCs are administered to the mouse. NIR illumination facilitates the real-time PA imaging of the MCs and subsequently triggers the propulsion of the micromotors in targeted areas of the GI tract. (ii) Schematic of PACT of the MCs in the GI tract in vivo. The mouse was kept in the water tank surrounded by an elevational focused ultrasound transducer array. NIR side illumination onto the mouse generated PA signals, which were subsequently received by the transducer array. (Inset) Enlarged view of the yellow dashed box region, illustrating the confocal design of light delivery and PA detection. US, ultrasound; CL, conical lens; DAQ, data acquisition system. (iii) Enteric coating prevents the decomposition of MCs in the stomach. (iv) External CW NIR irradiation induced the phase transition and subsequent collapse of the MCs on demand in the targeted areas and activated the movement of the micromotors upon unwrapping from the capsule. (v) Active propulsion of the micromotors promoted retention and cargo delivery efficiency in intestines. Middle panel (top and bottom): The stability of the MCs in gastric acid and intestinal fluid (top) without CW NIR irradiation and the use of CW NIR irradiation to trigger the collapse of an MC and the activation of the micromotors (bottom). Right panel: Time-lapse PACT images of the MCs in intestines for 7.5 h. The MCs migrating in the intestine are shown in color; the mouse tissues are shown in gray. Scale bar, 2 mm (reproduced with permission from Ref. [57], published by American Association for the Advancement of Science, 2019).

The resulting microrobots are covered by a red blood cell (RBC) membrane loaded with Staphylococcal α -toxin as a cargo model. The robots were then coated with chitosan, which was negatively charged to provide electrostatic interaction. Finally, the microrobot is packed in an enteric polymer, Eudragit L100–55, to protect the robot against acidic conditions (Figure 2D). Therefore, as previously mentioned, these robots can safely pass through the stomach and reach the intestine. The intestine environment is neutral, which can facilitate the dissolution of the polymeric layer and the activation of robots. They explored the interaction between the introduced microrobots and live cells and compared the result with static particles (without movement). The higher uptake of cells by active robots confirmed that propulsion enhances cell interaction. Finally, they evaluated the potency of the robot-based vaccine using a mouse model. One week after administration (orally), the antibody test was performed. The results reveal that the antitoxin IgA increased significantly, which shows that NMR technology helps deliver and retain antigenic payloads (Figure 2D).

However, as mentioned above, researchers have put much effort into the development of NMRs, imaging, positioning, and monitoring of NMR propulsion still remain the main challenges for biomedical in vivo application. In biomedical applications, optical imaging is a common tool, but difficulties arise when it is used for deep tissues. Due to light scattering, the image resolution drops significantly, which limits its application. In this regard, photoacoustic tomography (PAT) suggests deep tissue penetration, high resolution, and molecular contrast. Wu et al. [57] developed photoacoustic computed tomography-guided microrobots for gastrointestinal therapy.

Microrobots based on Mg were manufactured as previously reported (Figure 2E, left panel). The microrobots were then encapsulated in enteric polymer to survive in the acidic

environment of the stomach and passed to the intestines to propel and release the cargo. In the design of the microrobot, an Au layer was employed to increase light absorption for photoacoustic imaging. Therapeutic drugs and imaging agents were embedded in a hydrogel layer to provide maximum capacity. Microcapsules (encapsulated microrobots) can be activated using continuous-wave Near-infrared (NIR). The Au layer converts NIR light to heat, causing the release of microrobots from the capsule. This photothermal effect not only releases the microrobots but also accelerates the Mg–water reaction that results in higher speed propulsion (Figure 2E, middle panel). The function of the designed microrobots was examined using a mouse model for in vivo application. The Mg-based microrobot coated with enteric polymer was administered orally to the mouse. Twelve hours after administration, the retention of the Mg-based microrobot in the GI was evaluated. A much higher number of microrobots was retained compared with the passive particles. In the targeted drug delivery application (colon cancer), doxorubicin-loaded microrobots showed a higher release rate compared to capsules loaded with doxorubicin alone (Figure 2E, right panel).

2.3. CaO_2/Pt NPs Powered NMRs

Later, the research group of Zhang and Han introduced silica nanobottles (Si NBs) with a hydrophobic outer surface and a hydrophilic inner as a novel concept [54]. The hollow structure of Si NBs provides an efficient drug loading capacity. Clarithromycin (CLA), nano CaO_2 , and Pt NPs were loaded into Si NBs through amphiphilic interaction (Figure 3(Aa,b)). Upon delivery of the nanorobots to the stomach area, CaO_2 can react with gastric juice, consume protons, and produce hydrogen peroxide. The produced H_2O_2 could react with Pt NPs and drive the Si NB robots (Figure 3(Ac,d)). As Si NB robots propel in acid media by consuming the proton, the environment becomes neutral (Figure 3(Bi)). The cargo could be also released by ejecting bubbles due to the reaction between Pt NPs and produced H_2O_2 . Si NBs were administered orally to mice for five consecutive days and the in vivo toxicity profile was evaluated according to changes in body weight. The results confirm that there were no significant differences. In addition to body weight, blood biochemical analysis, gastrointestinal histopathology, and internal organ pathology have been performed to confirm the biosafety of the CLA/ CaO_2 /Pt@Si NB robots. The potential medical application of Si NBs for the treatment of *H. pylori* infection was examined using mouse models. The result of treatment with CLA/ CaO_2 /Pt@Si NB was compared with common oral treatment (PPI + CLA) and revealed that there were no significant differences between the two groups in terms of treatment; however, PPI was observed to cause severe damage to gastric cells. Interestingly, in the case of the stomach pH value of CLA/ CaO_2 /Pt@Si NB, the pH value returned to normal shortly, while for the group treated with PPI, this reverse was difficult. This could be the result of damage to gastric tissue cells caused by PPI (Figure 3(Bii–vi)).

2.4. Enzyme-Powered NMRs

Although Mg- and Zn-based NMRs have been successful in the treatment of GI diseases, there are still some challenges, such as their fuels and biodegradability. As the Mg/Zn catalytic reaction with the surrounding environment is aggressive, there is a potential for tissue damage. Another concern was raised about the retention of nondegradable residues in the stomach wall. For the treatment of stomach diseases, robot actuation is crucial. Therefore, alternative options are magnetized [7] or enzyme-based [5,58–60] NMRs with biocompatible reactions and complete biodegradability. Hahn et al. [55] developed bioinspired polydopamine (PDA) microrobots that used urea in the stomach as a biofuel for propulsion (Figure 4A,B). The silica microparticle was first covered by PDA polymerization, then the silica core was dissolved in HF solution, and the hollow polydopamine particles were placed in urease solution for immobilization via a Schiff base reaction. These microrobots hydrolyze urea using their conjugated urease and form ammonia and CO_2 . This propulsion facilitated the robot's penetration to the stomach wall. The in vivo experiment

(mice model) showed a remarkable improvement in penetration and prolonged retention in the stomach for one day. The microrobots disappeared after 3 days without causing any gastrointestinal tract toxicity (Figure 4C,D). This work demonstrated the feasibility of the potential use of stomach disease treatment using bioinspired and biodegradable microrobots [55].

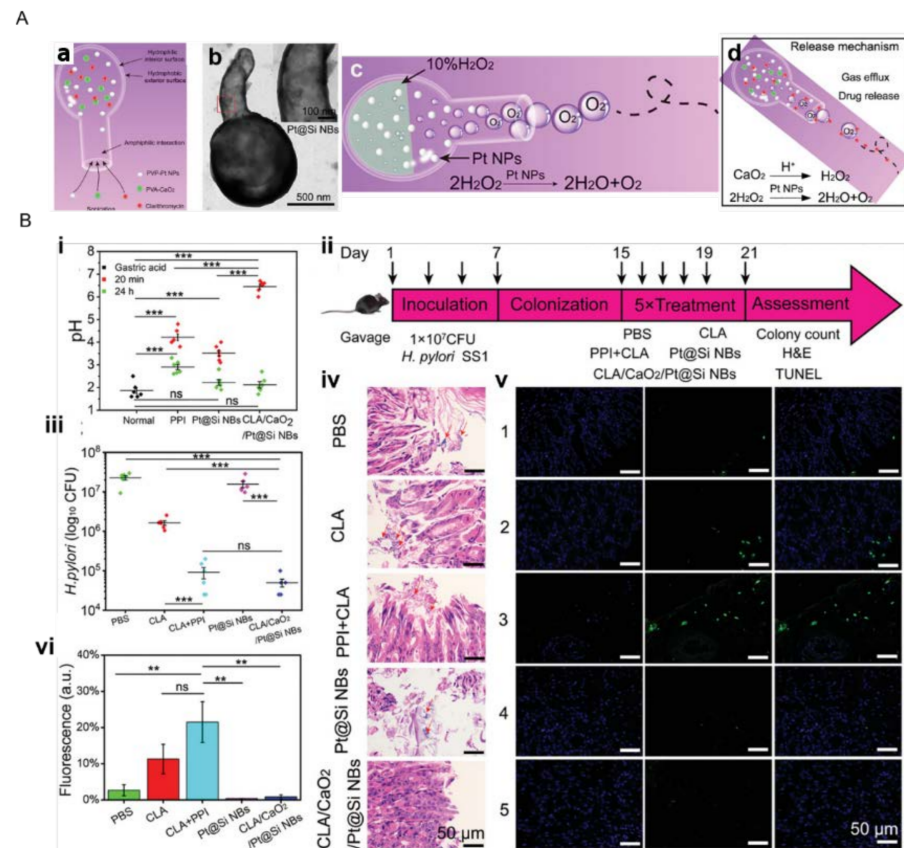


Figure 3. (A): (a) Selective loading of hydrophilic NPs on the interior surface of Si NBs. (b) TEM imaging of Pt@Si NBs. (c) Schematic diagram of the nanomotor driving mechanism. (d) Release mechanism of CLA. (B): *H. pylori*-infected treatment in vivo. (i) pH neutralization process at 20 min (red) and 24 h (green) after oral 400 $\mu\text{mol kg}^{-1}$ PPI, 15 mg Pt@Si NBs, and 15 mg CLA/CaO₂/Pt@Si NBs. (ii) Animal model treatment experiment process. (iii) Number of *H. pylori* in gastric tissue after different treatments. (iv) H&E staining and (v) the TUNEL staining of the stomach after different treatment (1. PBS, 2. CLA, 3. PPI + CLA, 4. Pt@Si NBs, 5. CLA/CaO₂/Pt@Si NBs). (vi) Quantitative evaluation of TUNEL staining (** $p < 0.01$, *** $p < 0.001$, ns, not significant) (reproduced with permission from Ref. [54], published by John Wiley and Sons, 2021).

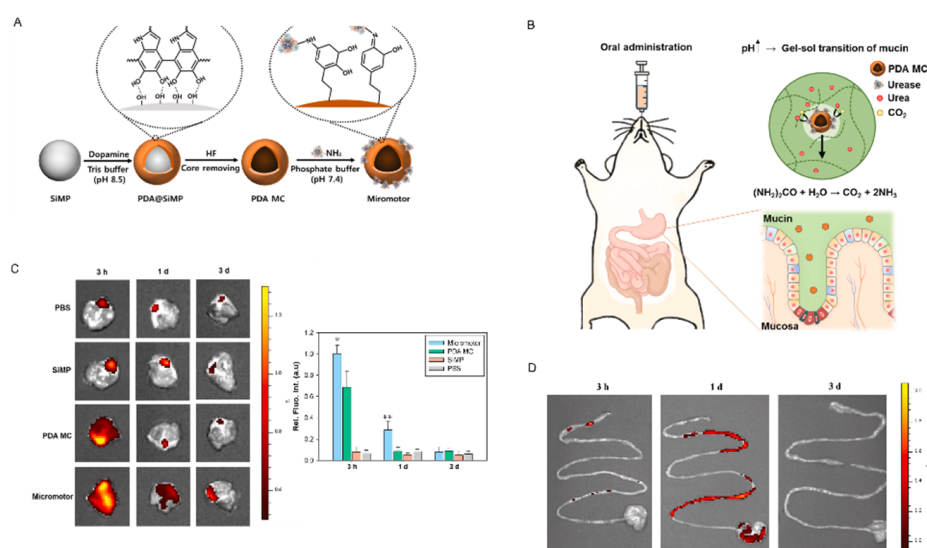


Figure 4. Schematic illustration for (A) the preparation procedure of urease-powered micromotors using silica microparticle (SiMP) and polydopamine microcapsule (PDA MC), and (B) the oral delivery of urease-powered polydopamine micromotors for enhanced penetration and retention in the stomach. (C) Left panel: IVIS images of the intact stomach at 3 h, 1 d and 3 d post-oral injection of PBS, SiMP, PDA MC and micromotors and right panel: the corresponding quantified fluorescence intensity at each time point ($n = 3$). (D) IVIS images of the intestinal tract at 3 h, 1 d, and 3 d post-oral administration of micromotors. (* $p \leq 0.05$, ** $p \leq 0.01$, micromotor vs. PDA MC) (reproduced with permission from Ref. [55], published by Elsevier, 2021).

2.5. Biohybrid NMRs

As mentioned above, one of the main challenges in NMR design is its biocompatibility. One of the solutions is to explore the nature database for biological units with inherited functionalities that can be employed in the design and engineering of the NMRs. The use of microorganisms such as sperm, neutrophils, algae, and bacteria in NMR design has been explored and promising results have been achieved [61,62]. Microalgae organisms have drawn much attention in the biomedical field as novel biological materials with inherent characteristics such as autofluorescent pigments, magnetic resonance signals, biodegradability, and low cytotoxicity [63,64]. Zhang et al. developed a microrobot based on *Spirulina platensis* (helical shapes) for active targeted delivery and imaging purposes in vivo [53,65]. They covered *Spirulina platensis* with Fe_3O_4 nanoparticles through a simple dip-coating process (Figure 5A). Integrating the Fe_3O_4 NPs into *Spirulina platensis* equipped them for remote actuation using an external magnetic field. They were able to swim in different media including DI water, blood, gastric juice, urine, and even peanut oil. As mentioned earlier, *Spirulina platensis* has instinct fluorescence, making it an ideal biomarker in biomedical applications. In this regard, their fluorescence stability was tested and the results reveal that over 60 min of illumination, the fluorescence was still stable, without any significant bleaching. Furthermore, the fluorescence signal was evaluated in different media such as neutral, alkaline, and acidic solutions, physiological media (containing 5% dextrose and phosphate-buffered saline), cell growth media, and isopropyl alcohol. The signal weakened only in acidic solution and IPA, while it remained without significant changes in the rest. The introduced microrobots have been used for in vivo imaging in (a) right below the dermis and (b) space between the parietal peritoneum and the visceral peritoneum of nude mice (Figure 5B). The results show that different factors contributed to the fluorescence signal, including (i) fluorescence characteristics, (ii) magnetization property, and (iii) an in situ environment. However, fluorescence-based biomedical imaging is a great help for the in vivo positioning of NMRs; it cannot penetrate deep tissues (more than few centimeters), which limits its application. One of the promising

methods for deep tissues is magnetic resonance imaging (MRI), as *Spirulina platensis* covered with Fe_3O_4 NPs can function as MR imaging contrast agents. The observed images revealed that the intensity of the contrast is a function of two factors: (a) concentration and (b) magnetization time. By prolonging the magnetization time, the imaging contrast could be significantly increased. The *Spirulina platensis* robots were tested for in vivo MR imaging in deep tissue (i.e., stomach) using a mouse model (Figure 5C). The results of the two different doses (4 mg/mL and 8 mg/mL) reveal that the MR contrasts depend on the concentration (4 mg/mL < 8 mg/mL).

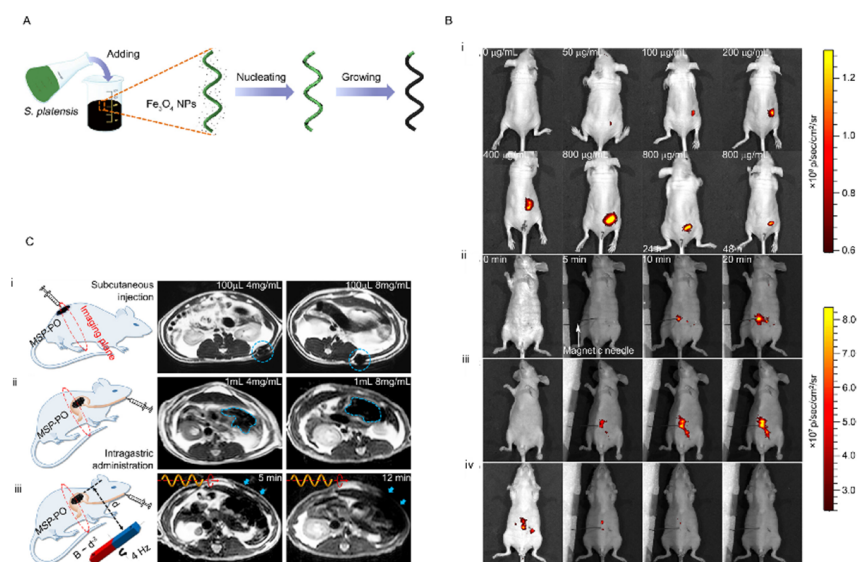


Figure 5. (A) Schematic of the dip-coating process of *S. platensis* in a suspension of Fe_3O_4 NPs. (B) (i) Fluorescence of 100 μL of MSP-72h with varying concentrations in the subcutaneous tissue of nude Balb/c athymic mice at three residence times. The residence time is 0 min unless otherwise specified. Fluorescence of 300 μL of (ii) MSP-72h, (iii) MSP-24h, and (iv) MSP-6h (all 800 $\mu\text{g}/\text{mL}$) in the intraperitoneal cavity at various residence times. Image sequences of (iii) and (iv) were recorded at the same time intervals with (ii). The magnetic needle was placed at $t = 3$ min. (C) (i) MSP swarm of two different concentrations inside the subcutaneous tissues. (ii) MSP swarm of two different concentrations inside the stomach. (iii) MSP swarm with the same concentration but subject to actuation and steering (with a rotating magnetic field) for different time periods before MR imaging across the rat's stomach (reproduced with permission from Ref. [53], published by American Association for the Advancement of Science, 2017).

3. Discussion and Conclusions

In this mini review, our objective was to explore the current status of the nano/micro-robots reported for stomach disease as an example of a targeted drug delivery application of NMRs (Table 1). In summary, the pioneering reports mentioned above administered micro-robots to the stomach/intestine of a living mouse, and then their distribution, retention, completeness of the task and toxicity profile were examined. Mg/Zn-based nano- and micro-robots have shown considerable promise for fast swimming through complex biological fluids, penetrating the walls of the stomach and intestines, and efficient delivery of therapeutic cargo to the targeted area with excellent biocompatibility. One of the main problems in targeted drug delivery is the retention of cargo carriers in the targeted region. These studies focused mainly on improving and prolonging the interactions between the particles and the mucoadhesive by either surface engineering or biofluid-driven propulsion of the active NMRs. For targeted drug delivery, either the payload can be released as the Mg/Zn body gradually dissolves in the specific environment, or the cargo can be embedded into an enteric stimuli-responsive polymer and then be released when the polymer responds to the environmental changes (e.g., pH, temperature, electric/magnetic field). One of the main features of these microrobots is the neutralization of their swimming environment.

The ability of NMRs to transfer and deliver different and multiple therapeutic drugs shows great promise in treating various disorders in the stomach or in different segments of the gastrointestinal tract efficiently and safely.

Currently, the introduced passive drug delivery platforms suffer from particle size limitations, complex design, low accuracy, and lack of specificity. The use of NMRs in drug delivery introduces an active and smart platform that is expected to solve the current difficulties that exist in passive drug delivery. The final goal is to introduce NMR-based platforms made of biocompatible materials that can be easily modified to carry different cargos (multidrug treatment), equipped with diagnostic sensors, and simply customized to any particle size. This active platform also needs to be precisely located and tracked during the delivery task. It would be preferred that NMRs actively create the desired environment in which it is necessary to activate the release without an external stimulus. Finally, long retention times and sustainable release profiles will be achieved by employing an NMR-based platform for targeted delivery. Although current platforms have been used for in vivo studies using small animals (mice), they may not translate easily to humans due to the complex system. Human clinical translation will be more complex and may require more sophistication. For example, as mentioned above, photoacoustic tomography (PACT) has been replaced by a fluorescence imaging technique for deep tissue imaging in mice. This technique can provide up to 7 cm tissue penetration, which in humans for deep tissue usually requires tens of centimeters of tissue penetration, which is limited by photon dissipation and needs to be replaced by a more penetrating excitation source. These changes may lead to a complete redesign of NMRs.

As discussed in this article, researchers in this field have made great progress, and advances in in vivo animal tests are considered an excellent step toward the realization of this technology; however, there are still key challenges that need to be addressed and overcome before employing NMRs in practical targeted drug delivery applications and human clinical tests. This list includes the engineering, design, and development of fuel-free, biocompatible, and self-destructive NMRs, the use of smart materials, a longer lifetime, higher loading capacity, and the programmable release of the therapeutic payload, which will be discussed in more detail.

3.1. Simple Fabrication and Easy Surface Modification

One of the major challenges that researchers are facing in the nano/microrobot field is the complexity and complications of synthesis. The fabrication methods either suffer from a scalability problem or require sophisticated technology, which in both cases is not appropriate for future clinical translation [66–68].

3.2. Biocompatibility and Biodegradability

Exploring novel, smart, functional, biocompatible and biodegradable materials and reactions, and also efficient biocompatible propulsion mechanisms for the motion of the NMRs are crucial for practical biomedical applications. For example, NMRs can potentially (i) accumulate in biological tissues, (ii) produce undesired reaction products (propulsion reaction), and (iii) be attacked by the immune system. Moreover, NMRs need to be easily and quickly degraded into nontoxic substances after completing their tasks. One ultimate solution is to make fully biodegradable NMRs that can self-destroy. It is also urgent to employ either fuel-free NMRs or explore biological fluids such as in situ fluids. However, as described here, some biofriendly NMRs such as Zn- and Mg-based NMRs have been developed for biomedical applications, but there are challenges that need to be explored further regarding the waste treatment of these catalysts and the exhausted gases [11,66,69,70].

3.3. Multifunctionality

In biomedical applications, it is necessary to combine several requirements for a specific application. For example, in the target delivery, not only is the high loading capacity of the carrier a matter, but it should also be able to release the loaded drug on

demand in response to internal or external stimuli. Furthermore, it must be located and tracked during drug delivery, so it is necessary to be equipped with the material used as an agent for bioimaging (this will be discussed further in imaging) [11].

3.4. Propulsion

Due to the complexity of the biological environment, precise remote powering, control, and real-time tracking of the NMRs are required. This control can be achieved using an internal body signal such as pH, temperature, biomolecules, and chemical gradient or an external source, that is, ultrasound, magnetic field, light, and electrical field. One of the main obstacles is adjusting the motion using an external source once the NMRs are operating in deep tissues. Table 2 lists the considerations that must be taken into account for external sources introduced and used in biomedical applications.

Table 2. Considerations must be taken into account for external sources introduced [10,68,70–73].

External Source	Considerations
Light	UV light damages the function of the immune system and living organisms. UV and visible light have a poor penetration ability into human tissues. X-ray has an adverse effect on human health (hair loss, increased possibility of cancer and genetic mutation, infertility). NMRs operating with high-power lasers may generate overheat in biological tissues. Light-driven NMRs usually cannot move in high-ionic-strength environments. Light-driven NMRs usually require a chemical fuel to trigger their activity, such as H ₂ O ₂ , which is toxic and cannot be used for medical applications.
Ultrasound	The choice of material is limited. Heat generation.
Magnetic field	Construction of a large magnetic field with precise control. Costly. Biocompatible magnetic materials should be employed to fabricate NMRs.
Electrical field	Safety concern. Electrodes are required to reach the potential and need to be close to the NMRs, which implies difficulties.

It is desired to design NMRs that can be self-propelled by sensing chemical gradients present in the body continuously, which means that the fabrication of these NMRs remains a challenge in its current status. Thus, it is vital to develop an efficient strategy to control and monitor the motion of NMRs. The difficulty increases once a group of NMRs is required to complete the biomedical task. Moreover, NMRs need a motion strategy with enough power to be able to move in vivo in biological media, and the flow also needs to be considered [66,70].

3.5. Lifetime

Usually, NMRs contain metals as catalysts that consume fuels and propel NMRs by producing bubbles. These catalysts are consumed rapidly, and this raises the question of whether NMR propulsion lasts enough for the designated task.

3.6. Imaging

Another major challenge for almost all in vivo NMRs is location and real-time tracking. The current solution is to employ bioimaging techniques such as optical fluorescence (FI), infrared emission, X-ray, radionuclide (RI), magnetic resonance (MRI), computed tomography (CT), positron emission tomography (PET), single-photon emission computed tomography (SPECT), photoacoustic computed tomography (PECT), or ultrasound (USI) imaging, which still have certain limitations in penetration, especially for deep tissue, precision, sensitivity, and tracking. Real-time tracking of NMRs in vivo remains a challenge

and needs to be explored further. Table 3 lists these difficulties at the current stage. To improve imaging efficiency, the combing technique could be a solution [11,66,74].

Table 3. The difficulties with bioimaging of NMRs at the current stage [23,24,66,70,72,74].

Imaging Technique	Consideration
FI	This technique requires embedding a fluorescent dye in the fabrication of NMRs without any change in their fluorescent characteristics. Most fluorescent dyes are toxic, and only a few are allowed to be used in biosystems. Fluorescent imaging is generally based on visible light, which cannot penetrate deep tissues because of weak power. In addition, they have poor stability in acid, salt, alkali, and other media. Self-quenching is also another concern.
MRI	Size limitation is the main challenge in using this technique. Moreover, magnetic resonance imaging is a slow imaging method that limits its application as a tracker in vivo.
RI	Safety issues due to exposure to ionizing radiation (X-rays and radionuclides).
USI	However, USI is considered a promising imaging method for in vivo application of NMRs, and USI still faces some limitations such as errors in locating artifacts and background signals. Moreover, it should be considered that USI is not an appropriate technique for the imaging of gas-containing organs.
PACT	Imaging depth is limited (several centimeters). The imaging speed is also limited due to the repetition rate of laser pulses

3.7. Size

Another factor that needs to be considered is the size of the designed NMRs. The smallest capillary in the human body is 5–10 μm . Therefore, the size of the designed NMRs needs to be significantly smaller. It is desired that the NMRs design is based on the application and can be easily fabricated in the required sizes for a specific task, including all the embedded components [66,70].

3.8. Immunogenicity

However, some biofriendly NMRs have been developed for in vivo applications, such as those explained in this mini review, and research on the toxicity of these materials in vivo is still limited to certain specific sites and is studied in the short term. This research does not provide long-term immune studies of the whole body [66,75].

4. Prospects and Future Direction

All of these constraints make the design and production of nanomotors/micromotors difficult for in vivo biomedical applications. Thus, despite the remarkable development of the bioapplication of NMRs in proof-of-concept studies, there is still a long way to go before their realization in vivo. This research field is multidisciplinary and requires the collaboration of scientists from different research areas such as chemistry, materials science, nanotechnology, catalysis, biology, medicine, and engineering. Moving toward the in vivo application of NMRs, the further development of biohybrid NMRs could cause a revolution in this technology and speed up the realization. Living microorganisms can convert chemical energy into physical work. In addition, they can respond to external stimuli and chemicals in the environment through biological sensing and interaction capabilities. They can hybridize with artificial components that provide a means to externally control and regulate their designated tasks and enhance their functionality. Hybrid NMRs are expected to be a solution to several challenges mentioned above, such as biocompatibility, biodegradability, propulsion, size, and safety. Another issue that will receive more attention is the integration of the NMRs with microfluidic. Exploring the NMRs inside the microfluidic chips is an essential step toward biomedical applications. It provides a platform to investigate the interactions between the robot, the fluid with other elements (proteins, particles, cells, or antibodies), and the surface.

In summary, this research community is expecting a nanorobot with proper size and fast propulsion which is made of biocompatible or biodegradable materials. This nanorobot is required to accomplish its specific task (for example, sense the tumor site, enter inside and release therapeutic agents) at the right time. The harm to the tissues/body should be as minimal as possible. Upon completion of the task, it needs to remove itself from the body.

Author Contributions: Conceptualization, B.K. and L.D.; literature review, B.K., L.D., J.L. and H.Z.; writing—original draft preparation, L.D., J.L. and H.Z.; writing—review and editing, B.K. and Z.S.; supervision, B.K. and Z.S. All authors have read and agreed to the published version of the manuscript.

Funding: Bahareh Khezri and Lukas Dekanovsky gratefully acknowledge the Czech Science Foundation (GACR no. 20-20201S). Jinhua Li acknowledges support from the European Structural and Investment Funds, the OP RDE-funded project ‘CHEMFELLS IV’ (No. CZ.02.2.69/0.0/0.0/20_079/0017899). Huaijuan Zhou sincerely acknowledges the financial support of the European Union’s Horizon 2020 research and innovation program under Marie Skłodowska-Curie grant agreement No. 890741.

Institutional Review Board Statement: Not applicable.

Informed Consent Statement: Not applicable.

Data Availability Statement: Not applicable.

Conflicts of Interest: The authors have no conflict of interest or financial ties to disclose.

References

1. Fleischer, R. *Fantastic Voyage*; 20th Century Fox: Los Angeles, CA, USA, 1966.
2. Feynman, R.P. There’s plenty of room at the bottom. *Resonance* **2011**, *16*, 890. [[CrossRef](#)]
3. Paxton, W.F.; Kistler, K.C.; Olmeda, C.C.; Sen, A.; St. Angelo, S.K.; Cao, Y.; Mallouk, T.E.; Lammert, P.E.; Crespi, V.H. Catalytic Nanomotors: Autonomous Movement of Striped Nanorods. *J. Am. Chem. Soc.* **2004**, *126*, 13424–13431. [[CrossRef](#)]
4. Arqué, X.; Romero-Rivera, A.; Feixas, F.; Patiño, T.; Osuna, S.; Sánchez, S. Intrinsic enzymatic properties modulate the self-propulsion of micromotors. *Nat. Commun.* **2019**, *10*, 2826. [[CrossRef](#)] [[PubMed](#)]
5. Dey, K.K.; Zhao, X.; Tansi, B.M.; Méndez-Ortiz, W.J.; Córdova-Figueroa, U.M.; Golestanian, R.; Sen, A. Micromotors Powered by Enzyme Catalysis. *Nano Lett.* **2015**, *15*, 8311–8315. [[CrossRef](#)] [[PubMed](#)]
6. Chen, C.; Karshalev, E.; Guan, J.; Wang, J. Magnesium-Based Micromotors: Water-Powered Propulsion, Multifunctionality, and Biomedical and Environmental Applications. *Small* **2018**, *14*, 1704252. [[CrossRef](#)]
7. Koleoso, M.; Feng, X.; Xue, Y.; Li, Q.; Munshi, T.; Chen, X. Micro/nanoscale magnetic robots for biomedical applications. *Mater. Today Bio* **2020**, *8*, 100085. [[CrossRef](#)] [[PubMed](#)]
8. Lee, J.G.; Al Harraq, A.; Bishop, K.J.M.; Bharti, B. Fabrication and Electric Field-Driven Active Propulsion of Patchy Microellipsoids. *J. Phys. Chem. B* **2021**, *125*, 4232–4240. [[CrossRef](#)]
9. Lu, X.; Shen, H.; Zhao, K.; Wang, Z.; Peng, H.; Liu, W. Micro-/Nanomachines Driven by Ultrasonic Power Sources. *Chem. Asian J.* **2019**, *14*, 2406–2416. [[CrossRef](#)]
10. Bunea, A.-I.; Martella, D.; Nocentini, S.; Parmeggiani, C.; Taboryski, R.; Wiersma, D.S. Light-Powered Microrobots: Challenges and Opportunities for Hard and Soft Responsive Microswimmers. *Adv. Intell. Syst.* **2021**, *3*, 2000256. [[CrossRef](#)]
11. Wan, M.; Li, T.; Chen, H.; Mao, C.; Shen, J. Biosafety, Functionalities, and Applications of Biomedical Micro/nanomotors. *Angew. Chem. Int. Ed.* **2021**, *60*, 13158–13176. [[CrossRef](#)]
12. Li, M.; Xi, N.; Wang, Y.; Liu, L. Progress in Nanorobotics for Advancing Biomedicine. *IEEE Trans. Biomed. Eng.* **2021**, *68*, 130–147. [[CrossRef](#)] [[PubMed](#)]
13. Parmar, J.; Vilela, D.; Villa, K.; Wang, J.; Sánchez, S. Micro- and Nanomotors as Active Environmental Microcleaners and Sensors. *J. Am. Chem. Soc.* **2018**, *140*, 9317–9331. [[CrossRef](#)]
14. Singh, V.V.; Wang, J. Nano/micromotors for security/defense applications. A review. *Nanoscale* **2015**, *7*, 19377–19389. [[CrossRef](#)]
15. Molinero-Fernández, Á.; Jodra, A.; Moreno-Guzmán, M.; López, M.Á.; Escarpa, A. Magnetic Reduced Graphene Oxide/Nickel/Platinum Nanoparticles Micromotors for Mycotoxin Analysis. *Chem. Eur. J.* **2018**, *24*, 7172–7176. [[CrossRef](#)] [[PubMed](#)]
16. Bulatov, E.; Khaiboullina, S.; dos Reis, H.J.; Palotás, A.; Venkataraman, K.; Vijayalakshmi, M.; Rizvanov, A. Ubiquitin-Proteasome System: Promising Therapeutic Targets in Autoimmune and Neurodegenerative Diseases. *BioNanoScience* **2016**, *6*, 341–344. [[CrossRef](#)]
17. Lin, R.; Yu, W.; Chen, X.; Gao, H. Self-Propelled Micro/Nanomotors for Tumor Targeting Delivery and Therapy. *Adv. Healthc. Mater.* **2021**, *10*, 2001212. [[CrossRef](#)]
18. Sun, M.; Fan, X.; Meng, X.; Song, J.; Chen, W.; Sun, L.; Xie, H. Magnetic biohybrid micromotors with high maneuverability for efficient drug loading and targeted drug delivery. *Nanoscale* **2019**, *11*, 18382–18392. [[CrossRef](#)]

19. Srivastava, S.K.; Clergeaud, G.; Andresen, T.L.; Boisen, A. Micromotors for drug delivery in vivo: The road ahead. *Adv. Drug Deliv. Rev.* **2019**, *138*, 41–55. [[CrossRef](#)]
20. Xu, H.; Medina-Sánchez, M.; Magdanz, V.; Schwarz, L.; Hebenstreit, F.; Schmidt, O.G. Sperm-Hybrid Micromotor for Targeted Drug Delivery. *ACS Nano* **2018**, *12*, 327–337. [[CrossRef](#)]
21. Luo, M.; Feng, Y.; Wang, T.; Guan, J. Micro-/Nanorobots at Work in Active Drug Delivery. *Adv. Funct. Mater.* **2018**, *28*, 1706100. [[CrossRef](#)]
22. Yim, S.; Gultepe, E.; Gracias, D.H.; Sitti, M. Biopsy using a magnetic capsule endoscope carrying, releasing, and retrieving untethered microgrippers. *IEEE Trans. Biomed. Eng.* **2014**, *61*, 513–521.
23. Gao, C.; Wang, Y.; Ye, Z.; Lin, Z.; Ma, X.; He, Q. Biomedical Micro-/Nanomotors: From Overcoming Biological Barriers to In Vivo Imaging. *Adv. Mater.* **2021**, *33*, 2000512. [[CrossRef](#)] [[PubMed](#)]
24. Van Moelenbroek, G.T.; Patiño, T.; Llop, J.; Sánchez, S. Engineering Intelligent Nanosystems for Enhanced Medical Imaging. *Adv. Intell. Syst.* **2020**, *2*, 2000087. [[CrossRef](#)]
25. Pané, S.; Puigmartí-Luis, J.; Bergeles, C.; Chen, X.-Z.; Pellicer, E.; Sort, J.; Počepcová, V.; Ferreira, A.; Nelson, B.J. Imaging Technologies for Biomedical Micro- and Nanoswimmers. *Adv. Mater. Technol.* **2019**, *4*, 1800575. [[CrossRef](#)]
26. Martella, D.; Nocentini, S.; Parmeggiani, C.; Wiersma, D.S. Photonic artificial muscles: From micro robots to tissue engineering. *Faraday Discuss.* **2020**, *223*, 216–232. [[CrossRef](#)] [[PubMed](#)]
27. Hu, C.-M.J.; Fang, R.H.; Copp, J.; Luk, B.T.; Zhang, L. A biomimetic nanosponge that absorbs pore-forming toxins. *Nat. Nanotechnol.* **2013**, *8*, 336–340. [[CrossRef](#)] [[PubMed](#)]
28. Wu, Z.; Li, T.; Gao, W.; Xu, T.; Jurado-Sánchez, B.; Li, J.; Gao, W.; He, Q.; Zhang, L.; Wang, J. Cell-Membrane-Coated Synthetic Nanomotors for Effective Biodetoxification. *Adv. Funct. Mater.* **2015**, *25*, 3881–3887. [[CrossRef](#)]
29. Pedram, A.; Pishkenari, H.N. Smart Micro/Nano-robotic Systems for Gene Delivery. *Curr. Gene Ther.* **2017**, *17*, 73–79. [[CrossRef](#)]
30. Hu, M.; Ge, X.; Chen, X.; Mao, W.; Qian, X.; Yuan, W.-E. Micro/Nanorobot: A Promising Targeted Drug Delivery System. *Pharmaceutics* **2020**, *12*, 665. [[CrossRef](#)]
31. Hwang, G.; Paula, A.J.; Hunter, E.E.; Liu, Y.; Babeer, A.; Karabucak, B.; Stebe, K.; Kumar, V.; Steager, E.; Koo, H. Catalytic antimicrobial robots for biofilm eradication. *Sci. Robot.* **2019**, *4*, eaaw2388. [[CrossRef](#)] [[PubMed](#)]
32. Lu, B.; Hu, E.; Xie, R.; Yu, K.; Lu, F.; Bao, R.; Wang, C.; Lan, G.; Dai, F. Magnetically Guided Nanoworms for Precise Delivery to Enhance In Situ Production of Nitric Oxide to Combat Focal Bacterial Infection In Vivo. *ACS Appl. Mater. Interfaces* **2021**, *13*, 22225–22239. [[CrossRef](#)]
33. Debraekeleer, A.; Remaut, H. Future perspective for potential *Helicobacter pylori* eradication therapies. *Future Microbiol.* **2018**, *13*, 671–687. [[CrossRef](#)] [[PubMed](#)]
34. Chi, Q.; Wang, Z.; Tian, F.; You, J.A.; Xu, S. A Review of Fast Bubble-Driven Micromotors Powered by Biocompatible Fuel: Low-Concentration Fuel, Bioactive Fluid and Enzyme. *Micromachines* **2018**, *9*, 537. [[CrossRef](#)] [[PubMed](#)]
35. Wang, Q.; Dong, R.; Wang, C.; Xu, S.; Chen, D.; Liang, Y.; Ren, B.; Gao, W.; Cai, Y. Glucose-Fueled Micromotors with Highly Efficient Visible-Light Photocatalytic Propulsion. *ACS Appl. Mater. Interfaces* **2019**, *11*, 6201–6207. [[CrossRef](#)]
36. Hortelao, A.C.; Simó, C.; Guix, M.; Guallar-Garrido, S.; Julián, E.; Vilela, D.; Rejc, L.; Ramos-Cabrer, P.; Cossío, U.; Gómez-Vallejo, V.; et al. Swarming behavior and in vivo monitoring of enzymatic nanomotors within the bladder. *Sci. Robot.* **2021**, *6*, eabd2823. [[CrossRef](#)]
37. Xu, C.; Wang, S.; Wang, H.; Liu, K.; Zhang, S.; Chen, B.; Liu, H.; Tong, F.; Peng, F.; Tu, Y.; et al. Magnesium-Based Micromotors as Hydrogen Generators for Precise Rheumatoid Arthritis Therapy. *Nano Lett.* **2021**, *21*, 1982–1991. [[CrossRef](#)]
38. Guo, M.; Wang, S.; Guo, Q.; Hou, B.; Yue, T.; Ming, D.; Zheng, B. NIR-Responsive Spatiotemporally Controlled Cyanobacteria Micro-Nanodevice for Intensity-Modulated Chemotherapeutics in Rheumatoid Arthritis. *ACS Appl. Mater. Interfaces* **2021**, *13*, 18423–18431. [[CrossRef](#)]
39. Wang, S.; Liu, K.; Zhou, Q.; Xu, C.; Gao, J.; Wang, Z.; Wang, F.; Chen, B.; Ye, Y.; Ou, J.; et al. Hydrogen-Powered Microswimmers for Precise and Active Hydrogen Therapy Towards Acute Ischemic Stroke. *Adv. Funct. Mater.* **2021**, *31*, 2009475. [[CrossRef](#)]
40. Blaser, M.J. *Helicobacter pylori* and the pathogenesis of gastroduodenal inflammation. *J. Infect. Dis.* **1990**, *161*, 626–633. [[CrossRef](#)] [[PubMed](#)]
41. Rotimt, O.; Nduduba, D.A.; Otegbeye, F.M. *Helicobacter pylori* and the pathogenesis of gastroduodenal disease: Implications for the management of peptic ulcer disease. *Niger. Postgrad. Med. J.* **2005**, *12*, 289–298. [[PubMed](#)]
42. Asaka, M.; Sugiyama, T.; Kato, M.; Satoh, K.; Kuwayama, H.; Fukuda, Y.; Fujioka, T.; Takemoto, T.; Kimura, K.; Shimoyama, T.; et al. A multicenter, double-blind study on triple therapy with lansoprazole, amoxicillin and clarithromycin for eradication of *Helicobacter pylori* in Japanese peptic ulcer patients. *Helicobacter* **2001**, *6*, 254–261. [[CrossRef](#)]
43. Tsay, F.-W.; Hsu, P.-I.H. *pylori* infection and extra-gastroduodenal diseases. *J. Biomed. Sci.* **2018**, *25*, 65. [[CrossRef](#)] [[PubMed](#)]
44. Sugiyama, A.; Maruta, F.; Ikeno, T.; Ishida, K.; Kawasaki, S.; Katsuyama, T.; Shimizu, N.; Tatematsu, M. *Helicobacter pylori* infection enhances N-methyl-N-nitrosourea-induced stomach carcinogenesis in the Mongolian gerbil. *Cancer Res.* **1998**, *58*, 2067–2069. [[PubMed](#)]
45. Kalisperati, P.; Spanou, E.; Pateras, I.S.; Korkolopoulou, P.; Varvarigou, A.; Karavokyros, I.; Gorgoulis, V.G.; Vlachoyiannopoulos, P.G.; Sougioultzis, S. Inflammation, DNA Damage, *Helicobacter pylori* and Gastric Tumorigenesis. *Front. Genet.* **2017**, *8*, 20. [[CrossRef](#)] [[PubMed](#)]

46. Jaynes, M.; Kumar, A.B. The risks of long-term use of proton pump inhibitors: A critical review. *Ther. Adv. Drug Saf.* **2018**, *10*, 2042098618809927. [[CrossRef](#)] [[PubMed](#)]
47. De Ávila, B.E.-F.; Angsantikul, P.; Li, J.; Angel Lopez-Ramirez, M.; Ramirez-Herrera, D.E.; Thamphiwatana, S.; Chen, C.; Delezuk, J.; Samakapiruk, R.; Ramez, V.; et al. Micromotor-enabled active drug delivery for in vivo treatment of stomach infection. *Nat. Commun.* **2017**, *8*, 272. [[CrossRef](#)]
48. Gao, W.; Dong, R.; Thamphiwatana, S.; Li, J.; Gao, W.; Zhang, L.; Wang, J. Artificial Micromotors in the Mouse's Stomach: A Step toward in Vivo Use of Synthetic Motors. *ACS Nano* **2015**, *9*, 117–123. [[CrossRef](#)]
49. Li, J.; Thamphiwatana, S.; Liu, W.; Esteban-Fernández de Ávila, B.; Angsantikul, P.; Sandraz, E.; Wang, J.; Xu, T.; Soto, F.; Ramez, V.; et al. Enteric Micromotor Can Selectively Position and Spontaneously Propel in the Gastrointestinal Tract. *ACS Nano* **2016**, *10*, 9536–9542. [[CrossRef](#)]
50. Li, J.; Angsantikul, P.; Liu, W.; Esteban-Fernández de Ávila, B.; Thamphiwatana, S.; Xu, M.; Sandraz, E.; Wang, X.; Delezuk, J.; Gao, W.; et al. Micromotors Spontaneously Neutralize Gastric Acid for pH-Responsive Payload Release. *Angew. Chem. Int. Ed.* **2017**, *56*, 2156–2161. [[CrossRef](#)]
51. Karshalev, E.; Esteban-Fernández de Ávila, B.; Beltrán-Gastélum, M.; Angsantikul, P.; Tang, S.; Mundaca-Uribe, R.; Zhang, F.; Zhao, J.; Zhang, L.; Wang, J. Micromotor Pills as a Dynamic Oral Delivery Platform. *ACS Nano* **2018**, *12*, 8397–8405. [[CrossRef](#)]
52. Esteban-Fernández de Ávila, B.; Lopez-Ramirez, M.A.; Mundaca-Uribe, R.; Wei, X.; Ramirez-Herrera, D.E.; Karshalev, E.; Nguyen, B.; Fang, R.H.; Zhang, L.; Wang, J. Multicompartment Tubular Micromotors Toward Enhanced Localized Active Delivery. *Adv. Mater.* **2020**, *32*, 2000091. [[CrossRef](#)]
53. Yan, X.; Zhou, Q.; Vincent, M.; Deng, Y.; Yu, J.; Xu, J.; Xu, T.; Tang, T.; Bian, L.; Wang, Y.-X.J.; et al. Multifunctional biohybrid magnetite microrobots for imaging-guided therapy. *Sci. Robot.* **2017**, *2*, eaaq1155. [[CrossRef](#)] [[PubMed](#)]
54. Wu, Y.; Song, Z.; Deng, G.; Jiang, K.; Wang, H.; Zhang, X.; Han, H. Gastric Acid Powered Nanomotors Release Antibiotics for In Vivo Treatment of *Helicobacter pylori* Infection. *Small* **2021**, *17*, 2006877. [[CrossRef](#)]
55. Choi, H.; Jeong, S.H.; Kim, T.Y.; Yi, J.; Hahn, S.K. Bioinspired urease-powered micromotor as an active oral drug delivery carrier in stomach. *Bioact. Mater.* **2021**, *9*, 54–62. [[CrossRef](#)]
56. Wei, X.; Beltrán-Gastélum, M.; Karshalev, E.; Esteban-Fernández de Ávila, B.; Zhou, J.; Ran, D.; Angsantikul, P.; Fang, R.H.; Wang, J.; Zhang, L. Biomimetic Micromotor Enables Active Delivery of Antigens for Oral Vaccination. *Nano Lett.* **2019**, *19*, 1914–1921. [[CrossRef](#)]
57. Wu, Z.; Li, L.; Yang, Y.; Hu, P.; Li, Y.; Yang, S.-Y.; Wang, L.V.; Gao, W. A microrobotic system guided by photoacoustic computed tomography for targeted navigation in intestines in vivo. *Sci. Robot.* **2019**, *4*, eax0613. [[CrossRef](#)] [[PubMed](#)]
58. Yuan, H.; Liu, X.; Wang, L.; Ma, X. Fundamentals and applications of enzyme powered micro/nano-motors. *Bioact. Mater.* **2021**, *6*, 1727–1749. [[CrossRef](#)]
59. Patiño, T.; Arqué, X.; Mestre, R.; Palacios, L.; Sánchez, S. Fundamental Aspects of Enzyme-Powered Micro- and Nanoswimmers. *Acc. Chem. Res.* **2018**, *51*, 2662–2671. [[CrossRef](#)] [[PubMed](#)]
60. Mathesh, M.; Sun, J.; Wilson, D.A. Enzyme catalysis powered micro/nanomotors for biomedical applications. *J. Mater. Chem. B* **2020**, *8*, 7319–7334. [[CrossRef](#)] [[PubMed](#)]
61. Alapan, Y.; Yasa, O.; Yigit, B.; Yasa, I.C.; Erkoc, P.; Sitti, M. Microrobotics and Microorganisms: Biohybrid Autonomous Cellular Robots. *Annu. Rev. Control Robot. Auton. Syst.* **2019**, *2*, 205–230. [[CrossRef](#)]
62. Lin, Z.; Jiang, T.; Shang, J. The emerging technology of biohybrid micro-robots: A review. *Bio-Des. Manuf.* **2021**. Available online: <https://link.springer.com/article/10.1007/s42242-021-00135-6#citeas> (accessed on 16 May 2021). [[CrossRef](#)]
63. Zhong, D.; Du, Z.; Zhou, M. Algae: A natural active material for biomedical applications. *VIEW.* **2021**. Available online: <https://onlinelibrary.wiley.com/doi/full/10.1002/VIW.20200189> (accessed on 23 February 2021).
64. Wang, H.-D.; Li, X.-C.; Lee, D.-J.; Chang, J.-S. Potential biomedical applications of marine algae. *Bioresour. Technol.* **2017**, *244*, 1407–1415. [[CrossRef](#)]
65. Yan, X.; Zhou, Q.; Yu, J.; Xu, T.; Deng, Y.; Tang, T.; Feng, Q.; Bian, L.; Zhang, Y.; Ferreira, A.; et al. Magnetite Nanostructured Porous Hollow Helical Microswimmers for Targeted Delivery. *Adv. Funct. Mater.* **2015**, *25*, 5333–5342. [[CrossRef](#)]
66. Wang, B.; Kostarelos, K.; Nelson, B.J.; Zhang, L. Trends in Micro-/Nanorobotics: Materials Development, Actuation, Localization, and System Integration for Biomedical Applications. *Adv. Mater.* **2021**, *33*, 2002047. [[CrossRef](#)]
67. Sun, J.; Tan, H.; Lan, S.; Peng, F.; Tu, Y. Progress on the fabrication strategies of self-propelled micro/nanomotors. *JCIS Open* **2021**, *2*, 100011. [[CrossRef](#)]
68. Liu, M.; Zhao, K. Engineering Active Micro and Nanomotors. *Micromachines* **2021**, *12*, 687. [[CrossRef](#)] [[PubMed](#)]
69. Wang, S.; Liu, X.; Wang, Y.; Xu, D.; Liang, C.; Guo, J.; Ma, X. Biocompatibility of artificial micro/nanomotors for use in biomedicine. *Nanoscale* **2019**, *11*, 14099–14112. [[CrossRef](#)]
70. Wang, W.; Zhou, C. A Journey of Nanomotors for Targeted Cancer Therapy: Principles, Challenges, and a Critical Review of the State-of-the-Art. *Adv. Healthc. Mater.* **2021**, *10*, 2001236. [[CrossRef](#)] [[PubMed](#)]
71. Soto, F.; Karshalev, E.; Zhang, F.; Esteban Fernandez de Avila, B.; Nourhani, A.; Wang, J. Smart Materials for Microrobots. *Chem. Rev.* **2021**. Available online: <https://pubs.acs.org/doi/10.1021/acs.chemrev.0c00999> (accessed on 1 February 2021). [[CrossRef](#)]
72. Wang, B.; Zhang, Y.; Zhang, L. Recent progress on micro- and nano-robots: Towards in vivo tracking and localization. *Quant. Imaging Med. Surg.* **2018**, *8*, 461–479. [[CrossRef](#)]

73. Wang, L.; Meng, Z.; Chen, Y.; Zheng, Y. Engineering Magnetic Micro/Nanorobots for Versatile Biomedical Applications. *Adv. Intell. Syst.* **2021**, *3*, 2000267. [[CrossRef](#)]
74. Aziz, A.; Pane, S.; Iacovacci, V.; Koukourakis, N.; Czarske, J.; Menciassi, A.; Medina-Sánchez, M.; Schmidt, O.G. Medical Imaging of Microrobots: Toward In Vivo Applications. *ACS Nano* **2020**, *14*, 10865–10893. [[CrossRef](#)]
75. Fu, D.; Wang, Z.; Tu, Y.; Peng, F. Interactions between Biomedical Micro-/Nano-Motors and the Immune Molecules, Immune Cells, and the Immune System: Challenges and Opportunities. *Adv. Healthc. Mater.* **2021**, *10*, 2001788. [[CrossRef](#)] [[PubMed](#)]